Ptychography: Theory & Algorithms

Albert Fannjiang

University of California, Davis

UC Irvine, June 10, 2021.

Fannjiang-Strohmer, *Acta Numerica* (2020), 125-228.

Coded-aperture phase retrieval

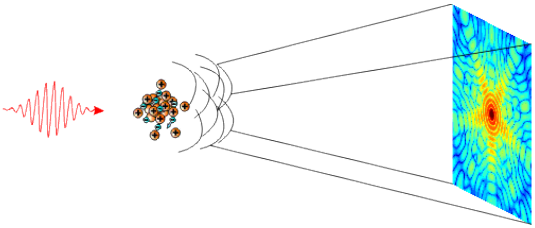

- Mask (wavefront) μ + propagation + intensity measurement:

$$\mu\text{-coded diffraction pattern} = |\Phi(f \odot \mu)|^2, \quad \Phi = \text{Fourier transform.}$$

- Ambiguities with one randomly coded diffraction pattern:

(harmless) constant phase	$f(\cdot) \longrightarrow e^{i\theta} f(\cdot)$
translation	$f(\cdot) \longrightarrow f(\cdot + \mathbf{n})$
conjugate inversion	$f(\cdot) \longrightarrow \bar{f}(-\cdot)$

Uniqueness theory

- Redundancy: 1+ randomly coded pattern.

Theorem (F. 2012)

Suppose f is a non-line object. Then the object is uniquely determined by two independent coded diffraction patterns up to a constant phase factor with probability one.

- Noise stability?
  $M \times N$ Gaussian measurement matrix: $M = \mathcal{O}(N)$
  - $\rightarrow$ Candes-Strohmer-Voroninski 2013, Candes-Li 2014, Demanet-Hand 2014, Hand 2017
  - $\rightarrow$ PhaseMax: Goldstein-Studer 2018, Dhifallah-Thrampoulidis-Lu 2017

Numerics

- (Empirical) global convergence
  - → Gradient-descent + special initialization methods: Alternating Projections (AP) or Wirtinger Flow (WF).
  - → Initialization methods:
    - – Spectral: Netrapalli-Jain-Sanghavi 2015, Chen-Candes 2017
    - – Null-vector: Chen-F.-Liu 2017
    - – Optimal spectral: Mondelli-Montanari 2019, Luo-Alghamdi-Lu 2019.

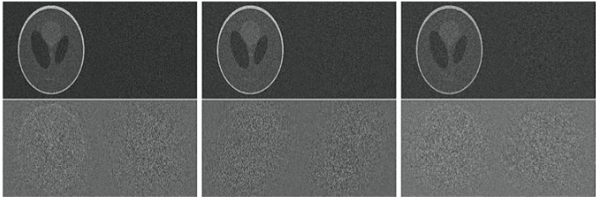

(a) NSR 0% (b) NSR 10% (c) NSR 20%

  - → Initialization methods are ineffective for blind phasing.

- ADMM/DRS: Globally and linearly convergent algorithm: Luke 2005, F.-Zhang 2020

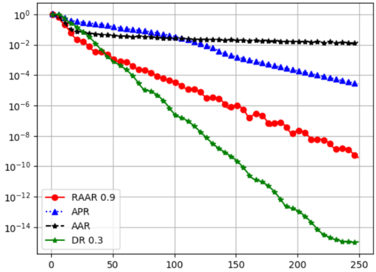

- Convergence proof:
  - → Local convergence for the Fourier case with two diffraction patterns (Chen-F.-Liu 2017, Chen-F. 2018).
  - → Global convergence for suboptimal algorithms: Li-Pong 2016.
  - → Global convergence for the Gaussian case with many diffraction patterns (Cand'es-Strohmer-Voroninski 2013, Candes-Li 2014, Candes-Li-Soltanolkotabi 2015).

Ptychography

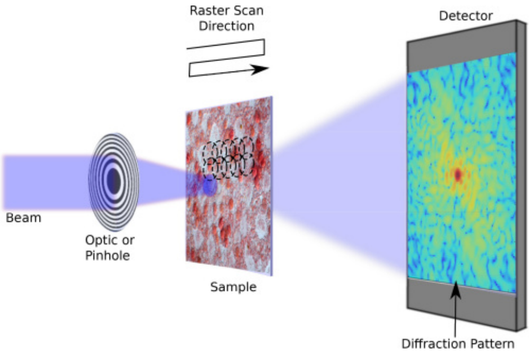

- Phase retrieval with windowed Fourier intensities.
- Measurement scheme:
  - → Window function?
  - → Scan pattern?
  - → Overlap?

Mask/probe retrieval

Thibault *et al.* 08/09

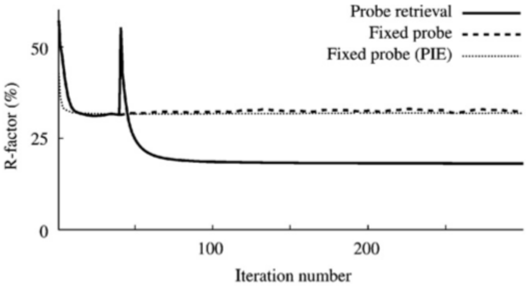

- Relative residual reduces (from 32% to 18%) after mask recovery routine is turned on.
- Simultaneous recovery of the mask and the object?

Maiden-Johnson-Li 2017

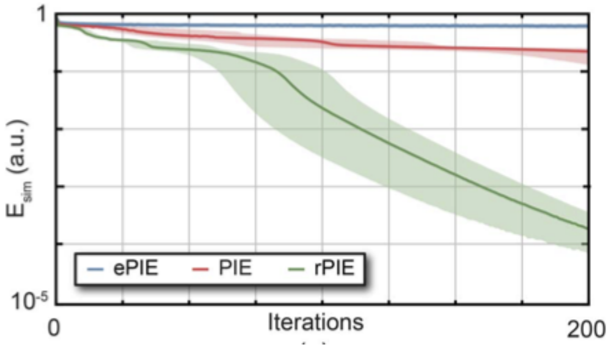

- The mask is randomly initialized and the object is initialized as a constant.
- Overlap ratio 70 – 80%.

Measurement scheme: notation & set-up

- $\mathcal{T}$: $\mathbf{t} \in \mathbb{Z}^2$ (pixel space) involved in ptychography.
- μ^0 the initial mask; $\mu^{\mathbf{t}}$ the $\mathbf{t}$-shifted mask
- $\mathcal{M}^0 = \mathbb{Z}_m^2$; $\mathcal{M}^{\mathbf{t}}$ the domain of $\mu^{\mathbf{t}}$.
- $\mathcal{M} := \cup_{\mathbf{t}\in\mathcal{T}} \mathcal{M}^{\mathbf{t}}$
- $f^{\mathbf{t}}$: the object restricted to $\mathcal{M}^{\mathbf{t}}$
- $\mathrm{Twin}(f^{\mathbf{t}})$: 180°-rotation of $\overline{f^{\mathbf{t}}}$ around the center of $\mathcal{M}^{\mathbf{t}}$
- $f = \vee_{\mathbf{t}} f^{\mathbf{t}}$ with support $\subseteq \mathcal{M}$.

The original object is broken up into a set of overlapping object parts, each of which produces a coded diffraction pattern (coded by $\mu^{\mathbf{t}}$).

Raster scan

Raster scan: $\mathbf{t}_{kl} = \tau(k, l), k, l \in \mathbb{Z}$ where τ is the step size.
$\mathcal{M} = \mathbb{Z}_n^2$, $\mathcal{M}^0 = \mathbb{Z}_m^2, n > m$, with the periodic boundary condition.

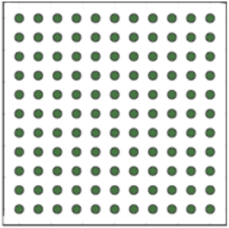

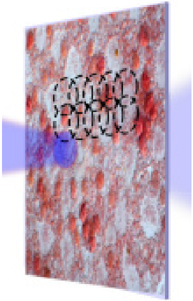

Measurement scheme

- $\mathcal{M}^{\mathbf{t}}$ = nodes
- Two nodes are s-connected if $|\mathcal{M}^{\mathbf{t}} \cap \mathcal{M}^{\mathbf{t}'} \cap \mathrm{supp}(f)| \geq s \geq 2$.

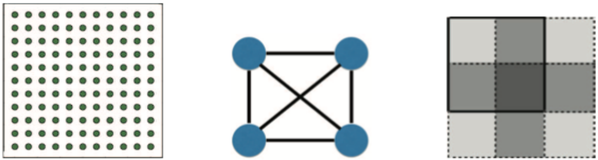

(a) raster scan (b) (c)

Theorem (Chen-F. 2017)

Suppose that ptychographic graph is s-connected ($s \geq 2$). If the known mask comprises non-vanishing independent continuous random variables and every object part $f^{\mathbf{t}}$ is non-line, then the object is uniquely, up to a constant phase factor, by the ptychographic data.

Iwen-Viswanathan-Wang 2016: Uniqueness for standard raster scan with a standard Gabor window function shifted by one pixel at a time.

Graph representation

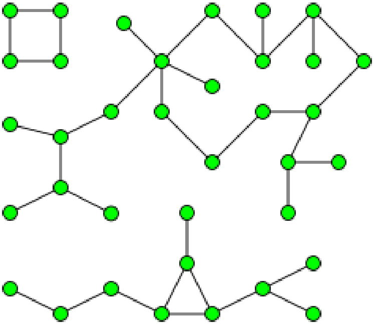

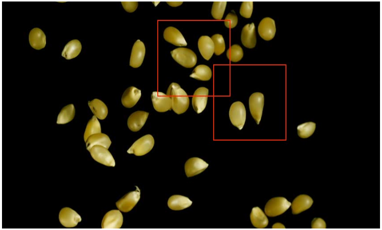

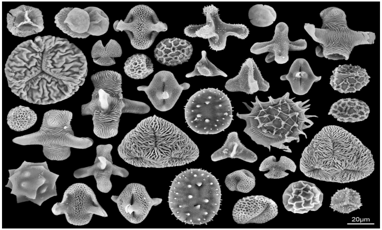

Raster scan with Fresnel mask can be ineffective

Twin-like ambiguity: Chen & F (2017)

Fresnel mask $\mu^0(\mathbf{k}) := \exp\{i\pi\rho|\mathbf{k}|^2/m\}$

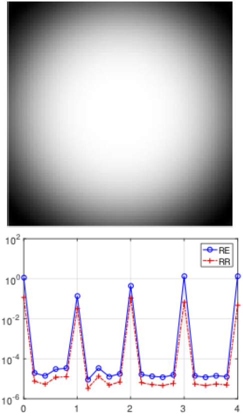

(a) $q = 2$

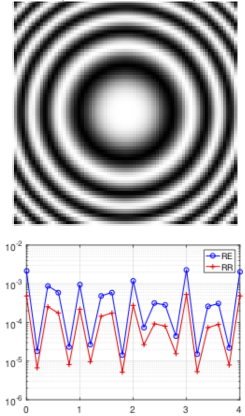

(b) $q = 4$

No uniqueness for a discrete set of ρ (except with one pixel shifts)!

Affine phase ambiguity

- Fundamental ambiguity with blind ptychography.
  Consider the probe and object estimates

$$\begin{aligned} \nu^0(\mathbf{n}) &= \mu^0(\mathbf{n})\exp(-\mathrm{i}a - \mathrm{i}\mathbf{w}\cdot\mathbf{n}), \quad \mathbf{n}\in\mathcal{M}^0 \\ g(\mathbf{n}) &= f(\mathbf{n})\exp(\mathrm{i}b + \mathrm{i}\mathbf{w}\cdot\mathbf{n}), \quad \mathbf{n}\in\mathbb{Z}_n^2 \end{aligned}$$

  for any $a, b \in \mathbb{R}$ and $\mathbf{w}\in\mathbb{R}^2$. Then

$$\nu^{\mathbf{t}}(\mathbf{n})g^{\mathbf{t}}(\mathbf{n}) = \mu^{\mathbf{t}}(\mathbf{n})f^{\mathbf{t}}(\mathbf{n})\exp(\mathrm{i}(b-a))\exp(\mathrm{i}\mathbf{w}\cdot\mathbf{t})$$

- $\exp(\mathrm{i}\mathbf{w}\cdot\mathbf{t})$ depends on $\mathbf{t}$ but not on $\mathbf{n}$ $\Rightarrow$ g and ν^0 produce the same ptychographic data as f and μ^0.

Phase drift

Necessary condition for blind ptychography:

$$(\star) \quad \nu^{\mathbf{t}} \odot g^{\mathbf{t}} = e^{\mathrm{i}\theta_{\mathbf{t}}} \mu^{\mathbf{t}} \odot f^{\mathbf{t}}, \quad \forall \mathbf{t} \in \mathcal{T},$$

for some $\theta_{\mathbf{t}}$ (phase drift).

Theorem (F 2019)

Let $\mathcal{T} = \{\mathbf{t}_k\}$ be a $\mathbf{v}$-generated cyclic group of order q and M^k the $\mathbf{t}_k$-shifted mask domain. Suppose that

$$\nu^k(\mathbf{n}) g^k(\mathbf{n}) = e^{\mathrm{i}\theta_k} \mu^k(\mathbf{n}) f^k(\mathbf{n}), \quad \textit{for all } \mathbf{n} \in \mathcal{M}^k \textit{ and } \mathbf{t}_k \in \mathcal{T}.$$

If

$$\mathcal{M}^k \cap \mathcal{M}^{k+1} \cap supp(f) \cap (supp(f) \oplus \mathbf{v}) \neq \emptyset, \quad \forall k$$

then $\{\theta_0, \theta_1, \ldots, \theta_{q-1}\}$ form an arithmetic progression.

Intermediate step

Theorem (F-Chen 2020)

Let the scheme be s-connected and each $f^{\mathbf{t}}$ is a non-line object. Suppose that some $f^{\mathbf{t}}$ has a tight support in $\mathcal{M}^{\mathbf{t}}$ and that $\mu^0 \neq 0$ has independently distributed random phases over at least the range of length π.

Suppose that ν^0 with

$$\text{(MPC)} \quad \Re\left[\overline{\nu^0}(\mathbf{n})\mu^0(\mathbf{n})\right] > 0, \quad \forall \mathbf{n} \in \mathcal{M}^0,$$

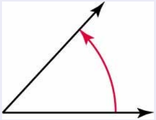

and an arbitrary object $g = \cup_k g^k$ produce the same ptychographic data as f and μ^0. Then the phase drift equation

$$(\star) \quad \nu^{\mathbf{t}} \odot g^{\mathbf{t}} = e^{\mathrm{i}\theta_{\mathbf{t}}}\mu^{\mathbf{t}} \odot f^{\mathbf{t}}, \quad \forall \mathbf{t} \in \mathcal{T},$$

holds with probability at least $1 - c^s$, $c < 1$, where c depends on the mask phase distribution.

Object support constraint (OSC)

$f^{\mathbf{t}}$ has a tight support in $\mathcal{M}^{\mathbf{t}}$: Each and every side of $\mathcal{M}^{\mathbf{t}}$ intersects with $\mathrm{supp}(f^{\mathbf{t}})$.

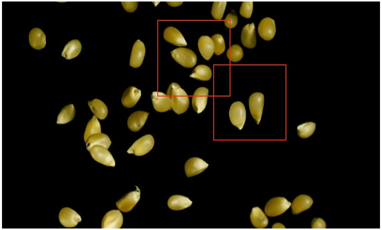

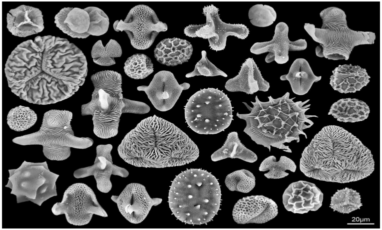

OSC for a measurement scheme (the scan pattern): any translation of f would move some nonzero pixels across $\cup_{\mathbf{t}} \partial \mathcal{M}^{\mathbf{t}}$.

OSC counter-example

Let $m = 2n/3$, $\mathbf{t} = (m/2, 0)$ $f^0 = [0, f_1^0]$ and $f^{\mathbf{t}} = [f_0^1, 0]$ with $f_1^0 = f_0^1$.
Likewise, $\mu^0 = [\mu_0^0, \mu_1^0]$, $\mu^{\mathbf{t}} = [\mu_0^1, \mu_1^1]$.
Let $\nu^0 = \mu^0, \nu^{\mathbf{t}} = \mu^{\mathbf{t}}$ and $g^0 = [g_0^0, 0], g^{\mathbf{t}} = [0, g_1^1]$ where

$$\begin{aligned} g^0(\mathbf{n}) &= \bar{f}^0(\mathbf{N} - \mathbf{n})\bar{\mu}^0(\mathbf{N} - \mathbf{n})/\mu^0(\mathbf{n}), \quad \forall \mathbf{n} \in \mathcal{M}^0 \\ g^{\mathbf{t}}(\mathbf{n}) &= \bar{f}^{\mathbf{t}}(\mathbf{N} + 2\mathbf{t} - \mathbf{n})\bar{\mu}^{\mathbf{t}}(\mathbf{N} + 2\mathbf{t} - \mathbf{n})/\mu^{\mathbf{t}}(\mathbf{n}), \quad \forall \mathbf{n} \in \mathcal{M}^{\mathbf{t}}. \end{aligned}$$

Hence $g^0 \odot \mu^0$ and $g^{\mathbf{t}} \odot \mu^{\mathbf{t}}$ produce the same diffraction patterns as $f^0 \odot \mu^0$ and $f^{\mathbf{t}} \odot \mu^{\mathbf{t}}$ but

$$\begin{aligned} g^0 \odot \mu^0 &\neq e^{i\theta_0} f^0 \odot \mu^0 \\ g^{\mathbf{t}} \odot \mu^{\mathbf{t}} &\neq e^{i\theta_{\mathbf{t}}} f^{\mathbf{t}} \odot \mu^{\mathbf{t}} \end{aligned}$$

even when the mask is completely known.

Block phase ambiguity

For $q = 3, \tau = m/2$, let

$$f = \begin{bmatrix} f_{00} & f_{10} & f_{20} \\ f_{01} & f_{11} & f_{21} \\ f_{02} & f_{12} & f_{22} \end{bmatrix}, \quad g = \begin{bmatrix} f_{00} & e^{i2\pi/3} f_{10} & e^{i4\pi/3} f_{20} \\ e^{i2\pi/3} f_{01} & e^{i4\pi/3} f_{11} & f_{21} \\ e^{i4\pi/3} f_{02} & f_{12} & e^{i2\pi/3} f_{22} \end{bmatrix}$$

be the object and its reconstruction, respectively, where $f_{ij}, g_{ij} \in \mathbb{C}^{n/3 \times n/3}$. Let

$$\mu^{kl} = \begin{bmatrix} \mu^{kl}_{00} & \mu^{kl}_{10} \\ \mu^{kl}_{01} & \mu^{kl}_{11} \end{bmatrix}, \quad \nu^{kl} = \begin{bmatrix} \mu^{kl}_{00} & e^{-i2\pi/3} \mu^{kl}_{10} \\ e^{-i2\pi/3} \mu^{kl}_{01} & e^{-i4\pi/3} \mu^{kl}_{11} \end{bmatrix}, \quad k, l = 0, 1, 2,$$

be the probe and its estimate, respectively, where $\mu^{kl}_{ij}, \nu^{kl}_{ij} \in \mathbb{C}^{n/3 \times n/3}$.

$\Longrightarrow \nu^{ij} \odot g^{ij} = e^{i(i+j)2\pi/3} \mu^{ij} \odot f^{ij}.$

Periodic ambiguity (raster grid pathology)

$(\tau = m/2)$ $\mathbf{t}_{kl}$-shifted probes μ^{kl} and ν^{kl} can be written as

$$\mu^{kl} = \begin{bmatrix} \mu^{kl}_{00} & \mu^{kl}_{10} \\ \mu^{kl}_{01} & \mu^{kl}_{11} \end{bmatrix}, \quad \nu^{kl} = \left[\epsilon \odot \mu^{kl}_{ij}\right]$$

Let

$$\epsilon = [\alpha(\mathbf{n})\exp(\mathrm{i}\phi(\mathbf{n}))], \quad \epsilon^{-1} = [\alpha^{-1}(\mathbf{n})\exp(-\mathrm{i}\phi(\mathbf{n}))] \in \mathbb{C}^{\tau\times\tau}.$$

Consider the two objects

$$f = \begin{bmatrix} f_{00} & \cdots & f_{q-1,0} \\ \vdots & \vdots & \vdots \\ f_{0,q-1} & \cdots & f_{q-1,q-1} \end{bmatrix}, \quad g = \left[\epsilon^{-1} \odot f_{ij}\right]$$

Two exit waves $\mu^{kl} \odot f^{kl}$ and $\nu^{kl} \odot g^{kl}$ are identical. But the estimates are far off.

Mixing schemes

- **Rank-one perturbation** $\mathbf{t}_{kl} = \tau(k, l) + (\delta_k^1, \delta_l^2)$.
- **Full-rank perturbation** $\mathbf{t}_{kl} = \tau(k, l) + (\delta_{kl}^1, \delta_{kl}^2)$.

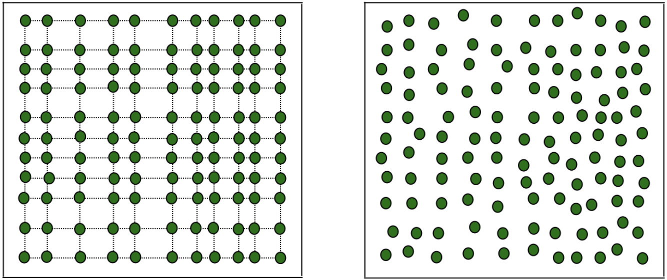

Global uniqueness

Theorem (F. 2019)

Suppose f does not vanish in $\mathbb{Z}_n^2$. Let $a_j^i = 2\delta_{j+1}^i - \delta_j^i - \delta_{j+2}^i$ and let $\{\delta_{j_k}^i\}$ be the subset of perturbations satisfying $\gcd_{j_k}\{|a_{j_k}^i|\} = 1, \quad i = 1, 2,$ *and*

$$\begin{aligned} \tau &\geq \max_{i=1,2}\{|a_{j_k}^i| + \delta_{j_k+1}^i - \delta_{j_k}^i\} \\ 2\tau &\leq m - \max_{i=1,2}\{\delta_{j_k+2}^i - \delta_{j_k}^i\}, \quad \text{(> 50\% overlap)} \\ m - \tau &\geq 1 + \max_{k'} \max_{i=1,2}\{|a_{j_k}^i| + \delta_{k'+1}^i - \delta_{k'}^i\}. \end{aligned}$$

Then APA and SF are the only ambiguities, i.e. for some explicit $\mathbf{r}$

$$\begin{aligned} g(\mathbf{n})/f(\mathbf{n}) &= \alpha^{-1}(0)\exp(\mathrm{i}\mathbf{n}\cdot\mathbf{r}), \\ \nu^0(\mathbf{n})/\mu^0(\mathbf{n}) &= \alpha(0)\exp(\mathrm{i}\phi(0) - \mathrm{i}\mathbf{n}\cdot\mathbf{r}) \\ \theta_{kl} &= \theta_{00} + \mathbf{t}_{kl}\cdot\mathbf{r}. \end{aligned}$$

Mixing schemes

Theorem (F.-Chen 2020)

If $\mathcal{T}$ satisfies the mixing property, then

$$
\begin{aligned}
g(\mathbf{n})/f(\mathbf{n}) &= \alpha^{-1}(0)\exp(\mathrm{i}\mathbf{n}\cdot\mathbf{r}), \\
\nu^0(\mathbf{n})/\mu^0(\mathbf{n}) &= \alpha(0)\exp(\mathrm{i}\phi(0)-\mathrm{i}\mathbf{n}\cdot\mathbf{r}) \\
\theta_{\mathbf{t}} &= \theta_0+\mathbf{t}\cdot\mathbf{r}.
\end{aligned}
$$

- Counterexamples exist for perturbed raster scans with $< 50\%$ overlap.
- Iwen-Preskitt-Saab-Viswanathan 2020: $\mathcal{T}=\mathbb{Z}_n^2 \Rightarrow$ noise stability.

Initialization with mask phase constraint

- Mask/probe initialization

$$\mu_1(\mathbf{n}) = \mu^0(\mathbf{n}) \exp\left[\mathrm{i}\phi(\mathbf{n})\right],$$

where $\phi(\mathbf{n})$ i.i.d. uniform on $(-\pi/2, \pi/2) \Longrightarrow$

$$\Re\left[\overline{\mu_1}(\mathbf{n})\mu^0(\mathbf{n})\right] > 0, \quad \forall \mathbf{n} \in \mathcal{M}^0,$$

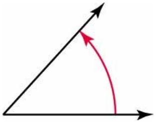

Relative error of the mask estimate

$$\sqrt{\frac{1}{\pi}\int_{-\pi/2}^{\pi/2} |e^{\mathrm{i}\phi} - 1|^2 d\phi} = \sqrt{2(1 - \frac{2}{\pi})} \approx 0.8525$$

- Object initialization: $f_1 =$ constant or random phase object.

Noise-aware ADMM

- Let $\mathcal{F}(\nu, x) =$ the totality of the Fourier (magnitude and phase) data for any mask ν and object x.
- Chang-Enfedaque-Marchesini 2019 consider the augmented Lagrangian

$$\mathcal{L}(\nu, x, z, \lambda) = \frac{1}{2}\|b - |z|\|^2 + \lambda^*(z - \mathcal{F}(\nu, x)) + \frac{\beta}{2}\|z - \mathcal{F}(\nu, x)\|^2$$

and the ADMM scheme

$$\begin{aligned}
\mu_{k+1} &= \arg\min \mathcal{L}(\nu, x_k, z_k, \lambda_k) \\
x_{k+1} &= \arg\min \mathcal{L}(\mu_{k+1}, x, z_k, \lambda_k) \\
z_{k+1} &= \arg\min \mathcal{L}(\mu_{k+1}, x_{k+1}, z, \lambda_k) \\
\lambda_{k+1} &= \lambda_k + \beta(z_{k+1} - \mathcal{F}(\mu_{k+1}, x_{k+1})).
\end{aligned}$$

Fourier domain algorithms

- F.-Strohmer 2020 considers the augmented Lagrangian

$$\mathcal{L}(y, z, \lambda) = \frac{1}{2}\||z| - b\|^2 + \lambda^*(z - y) + \frac{\rho}{2}\|z - y\|^2 + \mathbb{I}_{\mathcal{F}}(y)$$

where $\mathbb{I}_{\mathcal{F}}$ is the indicator function of $\{y : y = \mathcal{F}(\nu, x) \text{ for some } \nu, x\}$.

$$\Rightarrow \begin{cases} (z_{k+1}, \mu_{k+1}) &= \arg\min_z \mathcal{L}(y_k, z, x_k, \nu, \lambda_k) \\ (y_{k+1}, x_{k+1}) &= \arg\min_y \mathcal{L}(y, z_{k+1}, x, \mu_{k+1}, \lambda_k) \\ \lambda_{k+1} &= \lambda_k + \rho(z_{k+1} - y_{k+1}) \end{cases}$$

$$\Rightarrow \begin{cases} z_{k+1} &= \frac{1}{\rho+1} P_b(y_k - \lambda_k/\rho) + \frac{\rho}{\rho+1}(y_k - \lambda_k/\rho) \\ \mu_{k+1} &= B_k^+ y_k \\ y_{k+1} &= A_{k+1}A_{k+1}^+(z_{k+1} + \lambda_k/\rho) \\ x_{k+1} &= A_{k+1}^+ y_{k+1} \quad \text{(needed for } B_{k+1}\text{)} \\ \lambda_{k+1}/\rho &= \lambda_k/\rho + z_{k+1} - y_{k+1}. \end{cases}$$

where $A_\nu x := \mathcal{F}(\nu, x) =$ concatenation of $\{\Phi\,\mathrm{diag}(\nu^{\mathbf{t}})\}$ and $B_x\nu = \mathcal{F}(\nu, x) = \{\Phi\,\mathrm{diag}(x^{\mathbf{t}})\}$. Both have orthogonal columns.

eGaussian-DRS

In terms of the new variable $u_k = z_k + \lambda_{k-1}/\rho$, we have

$$
\begin{aligned}
u_{k+1} & \\
= \quad & \frac{1}{\rho+1} P_b(2A_k A_k^+ u_k - u_k) + \frac{\rho}{\rho+1}(2A_k A_k^+ u_k - u_k) + u_k - A_k A_k^+ u_k \\
= \quad & \frac{u_k}{\rho+1} + \frac{\rho-1}{\rho+1} A_k A_k^+ u_k + \frac{1}{\rho+1} P_b(2A_k A_k^+ u_k - u_k)
\end{aligned}
$$

with $\mu_{k+1} = B_k^+ A_k A_k^+ u_k, \quad x_{k+1} = A_{k+1}^+ u_{k+1}.$

Noise-agnostic ADMM

- Consider

$$\mathcal{L}(z,\nu,x,\lambda) = \mathbb{I}_b(z) + \lambda^*(z - \mathcal{F}(\nu,x)) + \frac{1}{2}\|z - \mathcal{F}(\nu,x)\|^2$$

and the following ADMM scheme

$$\begin{aligned} z_{k+1} &= \arg\min_z \mathcal{L}(z,\mu_k,x_k,\lambda_k) = P_b\left[\mathcal{F}(\mu_k,x_k) - \lambda_k\right] \\ (\mu_{k+1},x_{k+1}) &= \arg\min_\nu \mathcal{L}(z_{k+1},\nu,x,\lambda_k) \\ \lambda_{k+1} &= \lambda_k + z_{k+1} - \mathcal{F}(\mu_{k+1},x_{k+1}). \end{aligned}$$

- If we simplify the bilinear optimization step by one-step alternating minimization

$$\begin{aligned} \mu_{k+1} &= \arg\min_\nu \mathcal{L}(z_{k+1},\nu,x_k,\lambda_k) = B_k^+(z_{k+1} + \lambda_k) \\ x_{k+1} &= \arg\min_g \mathcal{L}(z_{k+1},\mu_{k+1},x,\lambda_k) = A_{k+1}^+(z_{k+1} + \lambda_k) \end{aligned}$$

then we obtain the DM algorithm of Thibault et al. 2008/2009.

eRAAR

Consider the augmented Lagrangian

$$\mathcal{L}(y,z,\nu,x,\lambda) \;=\; \mathbb{I}_Y(z) + \frac{1}{2}\|y - \mathcal{F}(\nu,x)\|^2 + \lambda^*(z-y) + \frac{\gamma}{2}\|z-y\|^2$$

$$\Rightarrow \begin{cases} (y_{k+1}, x_{k+1}) &= \arg\min_y \mathcal{L}(y, z_k, x, \mu_k, \lambda_k) \\ (z_{k+1}, \mu_{k+1}) &= \arg\min_z \mathcal{L}(y_{k+1}, z, x_{k+1}, \nu, \lambda_k) \\ \lambda_{k+1} &= \lambda_k + \gamma(z_{k+1} - y_{k+1}). \end{cases}$$

In terms of the new variable $u_{k+1} := y_{k+1} - \lambda_k/\gamma$ and $R_b = 2P_b - I$

$$\Rightarrow \begin{cases} u_{k+1} &= \beta u_k + (1-2\beta)P_b u_k + \beta P_k R_b u_k \\ \mu_{k+1} &= B^+_{k+1}(u_{k+1} + P_b u_k - u_k) \\ x_{k+1} &= A^+_k R_b u_k \end{cases}$$

Test objects and error metric

$+\ \imath$

$\times \exp \imath$

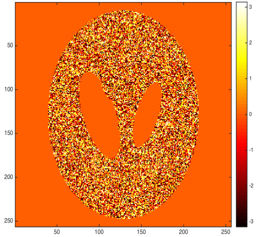

$$\mathrm{RE}(k) = \min_{\alpha \in \mathbb{C}, \mathbf{k} \in \mathbb{R}^2} \frac{\| f(\mathbf{r}) - \alpha e^{-\imath \frac{2\pi}{n} \mathbf{k} \cdot \mathbf{r}} f_k(\mathbf{r}) \|_2}{\| f \|_2}$$

Scan patterns

- Rank-one perturbation $\mathbf{t}_{kl} = 30(k, l) + (\delta_k^1, \delta_l^2)$ where δ_k^1 and δ_l^2 are randomly selected integers in $[-4, 4]$.
- Full-rank perturbation $\mathbf{t}_{kl} = 30(k, l) + (\delta_{kl}^1, \delta_{kl}^2)$ where δ_{kl}^1 and δ_{kl}^2 are randomly selected integers in $[-4, 4]$.
- The adjacent probes overlap by roughly 50%.
- Boundary conditions:

Periodic BC
Dark-field (enforced or not)
Bright-field (enforced or not)

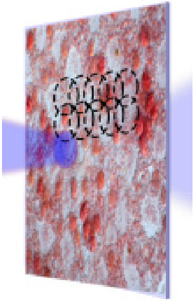

eGaussian-DRS vs eRAAR

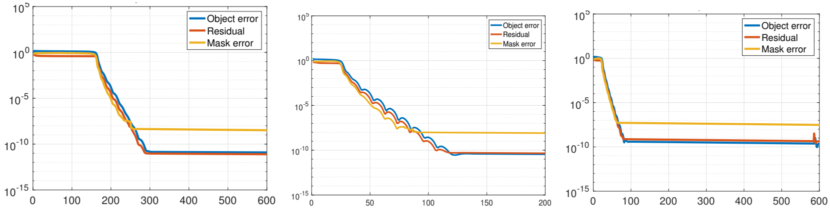

(a) 50% overlap; $\delta = 0.45$ (b) 66% overlap; $\delta = 0.4$ (c) 75% overlap; $\delta = 1/2$

Figure: eGaussian-DRS with $\rho = 1/3$ for CiB

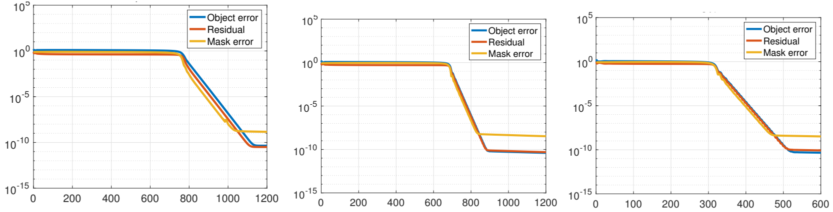

(a) 50% overlap; $\delta = 0.45$ (b) 66% overlap; $\delta = 0.4$ (c) 75% overlap; $\delta = 1/2$

Figure: eRAAR with $\beta = 0.8$ for CiB.

Local convexity

- Let $L(Ax) := \| b - |Ax| \|$ and $B = \mathrm{diag}\left[\mathrm{sgn}(\overline{Ax})\right] A$.

$$\begin{aligned}
\text{(gradient)} \quad 2\Re[\zeta^* \nabla L(Ax)] &= \Re(x^*\zeta) - b^\top \Re(B\zeta), \quad \forall \zeta \in \mathbb{C}^{n^2} \\
\text{(stationarity)} \quad B^*\left[|Ax| - b\right] &= 0 \\
\text{(Hessian)} \quad \Re[\zeta^* \mathrm{Hess}_x \zeta] &= \|\zeta\|^2 - \Im(B\zeta)^T \mathrm{diag}\left[\frac{b}{|Ax|}\right] \Im(B\zeta).
\end{aligned}$$

Theorem (Chen-F. 2018)

Suppose $f^{\mathbf{t}}$ is not a line object for any $\mathbf{t}$. For any connective scheme, the Hessian at $x = f$ (nonvanishing almost surely) is positive semi-definite and the eigenvalue zero has multiplicity one.

Proof: the second largest singular value λ_2 of

$$\mathcal{B} = \begin{bmatrix} -\Re(B) & \Im(B) \end{bmatrix}$$

is strictly less than 1 with probability one.

Gaussian-DRS with known mask

- Fourier domain fixed points: $P_X = AA^+, R_X = 2P_X - I$

$$P_X u + \rho P_X^\perp u = b \odot \text{sgn}(R_X u).$$

Theorem (F.-Zhang 2020)

Let u be a fixed point.
(i) $\rho \geq 1$: If u is attracting, then $|P_X u| = b$ (i.e. regular solution).
(ii) $\rho > 0$: If $|P_X u| = b$ then u is attracting.
(iii) $\rho = 0$: local linear convergence near the true object

- DRS ($\rho \geq 1$): A fixed point is linearly attracting iff it is a true solution.
- DR ($\rho = 0$): continuously distributed unstable fixed points in the vicinity of the true solution $\Longrightarrow$ sub-linearly attracting.
- Convergence rate achieves the minimum

$$\frac{\lambda_2}{\sqrt{1+\rho_*}} \quad \text{at} \quad \rho_* = 2\lambda_2\sqrt{1-\lambda_2^2} \in [0,1].$$

Conclusion and Questions

1. Blind ptychography not realizable with the regular raster scan:
   - → Mixing schemes: connective graph with overlap $\geq 50\%$
   - → Mask prior: mask phase constraint.

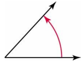

Extension: 3D tomographic phase retrieval with uncertain orientations.

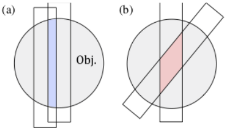

2. Local convergence analysis for Gaussian-DRS with known mask.
   Global convergence: cf. Li-Pong 2016.
   Noise leads to infeasible optimization problem:
3. Blind ptychography algorithms:
   - → Little convergence analysis: cf. Hesse-Luke-Sabach-Tam 2015
   - → Initialization method?

References I

- Cand‘es-Li 2014: “Solving quadratic equations via PhaseLift when there are about as many equations as unknowns”, *Found. Comput. Math.* **14**, 10171026.
- Cand‘es-Li-Soltanolkotabi 2015, “Phase retrieval from coded diffraction patterns”, *Appl. Comput. Harmon. Anal.* **39**, 277299.
- Cand‘es-Strohmer-Voroninski 2013: “PhaseLift: Exact and stable signal recovery from magnitude measurements via convex programming”, *Commun. Pure Appl. Math.* **66**, 12411274.
- Chen-Cand‘es 2017: “Solving random quadratic systems of equations is nearly as easy as solving linear systems”, *Commun. Pure Appl. Math.* **70**, 822-883.
- Chen-Chi-Fan-Ma 2019: “Gradient descent with random initialization: Fast global convergence for nonconvex phase retrieval”, *Math. Program.* **176**, 537.
- Chen-Fannjiang 2017: “Coded-aperture ptychography: Uniqueness and reconstruction,” *Inverse Problems* **34**, 025003.
- Chen-Fannjiang 2018, “Phase retrieval with a single mask by Douglas-Rachford algorithms,” *Appl. Comput. Harmon. Anal.* **44**, 665-699
- Chen-Fannjiang-Liu 2017: “Phase retrieval by linear algebra”. *SIAM Journal on Matrix Analysis and Applications* **38** 854-868.
- Chen-Fannjiang-Liu 2018: “Phase retrieval with one or two diffraction patterns by alternating projections with the null initialization”, *J. Fourier Anal. Appl.* **24**, 719-758.

Ref. II

- Demanet-Hand 2014, "Stable optimizationless recovery from phaseless linear measurements," *J. Fourier Anal. Appl.* **20**, 199-221.
- Fannjiang 2012: "Absolute uniqueness of phase retrieval with random illumination," *Inverse Problems* **28** 075008.
- Fannjiang 2019: "Raster Grid Pathology and the Cure" *Multiscale Model. Simul.* **17**, 973-995.
- Fannjiang-Chen 2020: "Blind ptychography: Uniqueness & ambiguities," *Inverse Problems* **36**, 045005.
- Fannjiang-Strohmer 2020, "The numerics of phase retrieval," *Acta Numerica*, 125-228.
- Fannjiang-Zhang 2020: "Blind Ptychography by Douglas-Rachford Splitting," *SIAM J. Imaging Sci.* **13**, 609-650.
- Hand 2017, "PhaseLift is robust to a constant fraction of arbitrary errors", *Appl. Comput. Harmon. Anal.* **42**, 550-562.
- Hesse-Luke-Sabach-Tam 2015, "Proximal heterogeneous block implicit-explicit method and application to blind ptychographic diffraction imaging," *SIAM J. Imaging Sci.* **8**, 426-457.
- Iwen-Preskitt-Saab-Viswanathan 2020: "Phase retrieval from local measurements: Improved robustness via eigenvector-based angular synchronization",*Appl. Comput. Harmon. Anal.* **48**, 415-444.

Ref. III

- Iwen-Viswanathan-Wang 2016: "Fast phase retrieval from local correlation measurements", *SIAM J. Imaging Sci.*, **9**, 1655-1688.
- Li-Pong 2016, "Douglas-Rachford splitting for nonconvex optimization with application to nonconvex feasibility problems", *Math. Program.* **A 159**, 371-401
- Luke 2005, "Relaxed averaged alternating reflections for diffraction imaging," *Inverse Problems* **21**, 37-50.
- Luo-Alghamdi-Lu 2019: "Optimal spectral initialization for signal recovery with applications to phase retrieval", *IEEE Trans. Signal Pro- cess.* **67**, 2347-2356.
- Maiden-Johnson-Li 2017: "Further improvements to the ptychographical iterative engine", *Optica*, **4**, 736-745.
- Mondelli-Montanari 2019: "Fundamental limits of weak recovery with applications to phase retrieval", *Found. Comput. Math.* **19**, 703-773.
- Netrapalli-Jain-Sanghavi 2015: "Phase retrieval using alternating minimization," *IEEE Transactions on Signal Processing* **63** 4814-4826.
- Thibault-Dierolf-Bunk-Menzel-Pfeiffer 2009: "Probe retrieval in ptychographic coherent diffractive imaging", *Ultramicroscopy* **109**, 338-343.
- Thibault-Dierolf-Menzel-Bunk-David-Pfeiffer 2008: "High-resolution scanning x-ray diffraction microscopy", *Science* **321**, 379-382.